

# Modular biomass gasification-based solid oxide fuel cells (SOFC) for sustainable development

Th. Seitarides, C. Athanasiou, A. Zabaniotou\*

*Chemical Engineering Department, Aristotle University of Thessaloniki, Un. Box 455, 54124 Thessaloniki, Greece*

Received 27 November 2006; accepted 22 January 2007

## Abstract

The integration of biomass gasification with SOFCs offers the potential of highly efficient and renewable power generation, primarily in modular solutions. SOFC seems to be the most promising fuel cell technology of biomass gasifier producer gases. Solid oxide fuel cells, because of their high operating temperature, do not require pure hydrogen as fuel, exhibiting high fuel flexibility. Sufficient amounts of cereal, cotton, corn, olive, coffee or palm tree residues are available in Mediterranean areas, while the climatic conditions are favorable for energy crops cultivations. Their residues can be utilized for electricity production by modular biomass gasification-based solid oxide fuel cells (SOFC).

© 2007 Elsevier Ltd. All rights reserved.

**Keywords:** Biomass gasification; Solid oxide fuel cells; Integration; Modeling

## Contents

1. Introduction . . . . .	1252
2. Gasification. . . . .	1253
2.1. Fluidized bed air and/or steam gasification . . . . .	1256
3. Fuel cells . . . . .	1258
3.1. Fuel cell types. . . . .	1258
3.1.1. Alkaline fuel cells . . . . .	1258
3.1.2. Polymer electrolyte membrane fuel cells . . . . .	1259

\*Corresponding author. Tel.: +30 2310996274; fax: +30 2310996209.

E-mail address: [sonia@cheng.auth.gr](mailto:sonia@cheng.auth.gr) (A. Zabaniotou).

3.1.3.	Phosphoric acid fuel cells . . . . .	1259
3.1.4.	Molten carbonate fuel cells . . . . .	1260
3.1.5.	Solid oxide fuel cells . . . . .	1261
3.2.	Thermodynamic analysis . . . . .	1263
3.2.1.	Chemical thermodynamics . . . . .	1264
3.2.2.	Steam reforming . . . . .	1270
4.	Discussion and potential impact of integrated BG-SOFC process . . . . .	1271
5.	Conclusions . . . . .	1272
	Acknowledgments . . . . .	1273
	References . . . . .	1273

---

## 1. Introduction

The main parameter concerning the integration of fuel cells technology in thermochemical processes of biomass conversion is the sufficient heat energy production in the cell in order to cover the thermal requirements of the thermochemical conversion of biomass. Several research groups have studied solid oxide fuel cells (SOFC) fuel flexibility, using theoretical analysis [1–9]. Thermodynamic simulation, supported by experimental investigation of a variety of fuels in a 25 kW tubular SOFC, has been reported by Singhal in 2000 [10]. Furthermore, Alderucci [11] carried out a thermodynamic study of a gasifier integrated to an SOFC and Kendall [12] powered a small tubular SOFC with simulated biogas.

Few studies concerning  $H_2$  production reported power densities reduced to the 1/3 of the corresponding values, mostly due to the dilution of the combustible agents [13]. Thus, Sulzer and Hexis have reported efficiencies close to 27% LHV, of a 1 kW SOFC, operating for 2,500 h on bio-derived gas [12,13], which is almost 1/2 of the regular SOFC efficiencies on  $H_2$  or reformed natural gas. Bin Zhu [14] reported power densities reduced almost equally to the  $H_2$  dilution (45% reduction for 45% dilution), in an innovative cell involving a mixed conducting electrolyte [14]. Apart from these studies, most of which refer to bio-derived gases and the contiguous landfill gas, there is a shortage of relevant data in literature.

Modeling studies of bio-derived gas utilization in SOFCs predicted efficiencies from 23% to 50% [13,15–17], the latest for theoretical fuel utilizations as high as 80%. Such utilization is achievable in  $H_2$  or  $CH_4/H_2O$  SOFCs, in which open-circuit voltages can exceed  $-1.2$  V, allowing operation at over potentials as high as  $0.8$  V, with almost optimum power densities [15,18]. This is hardly the case for bio-derived gas, for which the open-circuit voltage might not even reach  $-0.6$  V, and the optimum operational over potential is not greater than  $0.4$  V [19].

Due to the rapidly increased interest for SOFC-biomass conjunction, several pilot efforts of modular, biogas fed, SOFCs are currently under development for demonstration and investigation purposes. Moreover, SOFC integration to thermochemical biomass conversion systems can overbalance the heat requirements for gasification and suggest several thermal management challenges, in order to optimize the overall electrical efficiency. SOFC modules in the range of 1 kWel–1 MWel are already in demonstrative operation and therefore technologically available to potentially cover a wide range of biogas power sites.

In these cases, along with the inherent ability of SOFCs to keep the anode and cathode exhaust gases separate, which allows SOFC over-fuelling and adding downstream operations for the anode exhaust gases (gas or steam turbines), DOE wishes primarily to explore cell efficiencies on biogas and thermal integration issues.

A thermally integrated biomass-SOFC gasification system was designed by the University of North Dakota. The system uses a modified downdraft gasifier and is designed such that the high-energy effluents from the SOFC are recycled to the gasifier for heat recovery, which increases the biomass-to-gas conversion efficiency. Based on preliminary analysis, biomass-to-electricity conversion efficiencies up to 45% (higher heating value) were achieved [20]. Agricultural residues will be a key element in the bioeconomy as will a variety of energy and other crops. Rural development is both a significant benefit and a necessary component of a mature and integrated bioeconomy.

The combination of biomass with fuel cells emerged recently, could be a beneficiary candidate for decentralized and renewable heat and power cogeneration.

Distributed energy resources (DER) are small, modular, decentralized, grid-connected or off-grid power-generating systems located in or near the place where energy is used. These integrated power systems can include effective means of energy storage and delivery as well as power-generating technologies. DER systems can help to meet increased demand, reduce peak operating costs and improve the reliability of the electric power-generation system. Coupling DER systems with energy efficiency measures and good energy management practices can make them even more effective.

In the frame of a project going on in our laboratory, concerning sustainable development of non-European Mediterranean countries, research is on going whether modular biomass gasification/SOFC systems could provide renewable energy to remote areas and be served for the sustainable water management desalination systems.

## 2. Gasification

Concerning thermochemical processes, a number of reviews cover the principles and practices of catalytic gasification reporting higher efficiency and carbon conversion, elimination of condensable organics and enhanced economic viability, compared to non-catalytic processes [21–24]. Biomass gasification is the thermal conversion of organically derived, carbonaceous solid fuels into a gaseous energy medium, consisting primarily of hydrogen ( $H_2$ ) and carbon monoxide (CO) by adding oxygen, air, steam or combination of them as an oxidant. Smaller amounts of carbon dioxide ( $CO_2$ ), methane ( $CH_4$ ), ethane ( $C_2H_6$ ), water ( $H_2O$ ), nitrogen ( $N_2$ ) with air as an oxidant and a variety of contaminants such as carbon particulates, tar, ash and higher hydrocarbons are also present in the producer gas. On an atomic scale, biomass materials are made of mainly carbon, hydrogen, oxygen and nitrogen. Additionally, sulfur, chlorine, alkali metals and also heavy metals are present in varying quantities. The ultimate analysis of a biomass fuel involves determining the percentage of carbon, hydrogen, nitrogen, sulfur, chlorine and ash and calculating the percentage of oxygen by difference. The ultimate analysis of a fuel is essential in determining the theoretical air-to-feed ratio, the higher heating value of the biomass material and in assessing the pollution potential of the feedstock. Table 1 summarizes data from ultimate analysis of several dry ash-free biomass materials [27,28].

Heating value is the amount of energy released upon combustion of a unit mass of fuel. The two major factors affecting the heating value of biomass materials are ash

Table 1  
Ultimate analysis of different crop residues

Material	C	H	O	N	S	Ash	Ref.
Rice husk	38.3	4.36	35.45	0.83	0.06	21.00	[25]
Rice straw	41.80	4.60	36.60	0.70	0.08	15.90	[25]
Rice straw	41.8	4.63	36.6	0.70	0.08	13.4	[26]
Maize straw	47.09	5.54	39.79	0.81	0.12	5.77	[25]
Wheat straw	44.3–46.0	5.0–5.9	43.8–44.8	0.3–1.2	0.08–0.13	2.9–5.0	[25]
Wheat straw	47.2	6.20	42.00	0.80	0.13	3.70	[25]
Barley straw	44.5–46.0	5.1–5.6	41.6–44.6	0.2–0.8	0.10–0.19	4.0–7.4	[25]
Barley straw	47.50	6.30	41.70	0.60	0.07	3.80	[25]
Barley straw	46.8	5.53	41.9	0.41	0.006	4.9	[26]
Bagasse	46.95	6.10	42.65	0.30	0.10	3.90	[25]
Olive tree prunings	49.9	6	43.4	0.7	—	4.75	[26]
Cotton stalks	41.23	5.03	34	2.63	0	13.3	[26]
Corn stalks	45.53	6.15	41.11	0.78	0.13	6.4	[26]
Vineyard prunings	47.6	5.6	41.1	1.8	0.08	3.8	[26]
Corn cobs	46.3	5.6	42.19	0.57	0	5.34	[26]
Sugar beet leaves	44.5	5.9	42.8	1.84	0.13	4.8	[26]
Peach tree prunings	53	5.9	39.1	0.32	0.05	1	[26]
Oats straw	46	5.91	43.5	1.13	0.015	4.9	[26]
Sunflower straw	52.9	6.58	35.9	1.38	0.15	3	[26]
Apricot tree prunings	51.4	6.29	41.2	0.8	0.1	0.2	[26]

composition and moisture content. High values of these two components lower the heating value of biomass materials. The higher heating value is the amount of heat released from the combustion of a unit mass of fuel if all the water in the products exits at a steady flow in a condensed state. The lower heating value measures the amount of heat released from the combustion of a unit mass of fuel if all the products including water exit at a steady flow in a gaseous state [27]. Table 2 summarizes the lower and higher heating values of various crop residues [27–29].

If air or oxygen is used as an oxidant, the oxidation reactions can supply the heat necessary for covering the endothermic stages, thus no external energy supply is needed (autothermal gasification). If air is used as oxidizing agent, the producer gas will contain significant amounts of  $N_2$  (up to 50% vol.) due to the nitrogen content of air [25,30–33]. The nitrogen content in the producer gas may, therefore, be significantly reduced by using steam or oxygen as oxidizing agent. Due to the high nitrogen content in the producer gas, air gasification produces a low heating value gas of 4–6 MJ/Nm<sup>3</sup> (HHV) [33]. Oxygen and steam gasification on the other hand may produce a medium heating value (MHV) gas of 10–18 MJ/Nm<sup>3</sup> (HHV) [34].

Gasification occurs in a number of sequential steps [30,31,33]: *drying*: vaporization of the moisture content; *pyrolysis*: release of volatile matter (gas, vaporized tars or oils) and a solid char residue; *gasification*: partial oxidation of the char and heterogeneous reactions with  $CO_2$ ,  $H_2O$ ; *gas phase reactions*: reactions of the gaseous components formed in the first stages.

There are two basic gasification reactor types: the fixed bed gasifier and the fluidized bed gasifier with variations within each type. A third type, the entrained suspension gasifier,

Table 2

Lower heating value (LHV) and higher heating value (HHV) of various crop residues

Crop residue	LHV (MJ/Kg)	HHV (MJ/Kg)	Ref.
Rice husk	—	12.8–14.9	[27]
Rice straw	15.3	16.3	[27]
Wheat straw	16.5	17.5	[27]
Barley straw	18.2–19.4	17.1–18.2	[27]
Olive tree prunings	—	18.86	[29,28]
Cotton stalks	—	15.81	[29,28]
Durum wheat straw	—	17.92	[29,28]
Corn stalks	—	17.82	[29,28]
Soft wheat straw	—	17.92	[29,28]
Vineyard prunings	—	16.81	[29,28]
Corn cobs	—	18.02	[29,28]
Sugar beet leaves	—	17.72	[29,28]
Rice straw	—	12.16	[29,28]
Peach tree prunings	—	18.86	[29,28]
Almond tree prunings	—	18.43	[29,28]
Oats straw	—	18.11	[29,28]
Sunflower straw	—	20.83	[29,28]
Cherry tree prunings	—	21.78	[29,28]
Apricot tree prunings	—	20.83	[29,28]

has been developed for coal gasification but the need for a finely divided feed material ( $<0.1\text{--}0.4\text{ mm}$ ) presents problems for fibrous materials such as wood, which make the process largely unsuitable for most biomass materials and, therefore, the process is not considered further. The most commonly used among these are fixed bed and fluidized bed gasifiers.

Fixed bed gasifiers are employed in the low-capacity range of some  $\text{MW}_{\text{th}}$ , fluidized bed installations, typically in the range above  $5\text{ MW}_{\text{th}}$ . The fluidized bed types can be divided into bubbling and circulating systems. An additional distinction with gasifiers is made between pressurized and atmospheric installations [33]. The term gasification is used for the heterogeneous gas/char reactions and for the overall process in the gasifier, including all the mentioned sub-processes. In a fixed-bed gasification reactor, these sub-processes are spatially separated and can be assigned to layers, which are relatively clearly distinguished.

A fluidized bed gasifier comprises a fluidized bed of hot (often sand) particles, which are not consumed during the gasification process. Biomass is fed directly into or on top of the sand bed. Air is used as the fluidization medium and as a gasification medium. Generally, the four steps for the conversion of the biomass (drying, pyrolysis, combustion and gasification) cannot be clearly separated as in a fixed bed gasifier.

In a fluidized bed biomass gasifier, biomass particles are fed directly into or on top of a bed of sand. The high heat-transfer rate (approx.  $400\text{ W/m}^2\text{ K}$ ) from the hot fluidized bed particles to a biomass particle ensures rapid heating [35]. The biomass particle will go through a drying and pyrolysis process. These processes are accompanied by the gas production inside the particle. The processes yield permanent gases, primary and secondary tars and char as the main products. Drying and pyrolysis process inside the particle is hardly influenced by the gas composition surrounding the particle, as gases from outside hardly penetrate into the particle [36].

A review [35] of gasifier manufacturers in Europe, USA and Canada concluded that 75% of the designs were downdraft type, 20% of the designs were fluidized bed systems, 2.5% of the designs were updraft type and 2.5% were of various other designs.

2.1. Fluidized bed air and/or steam gasification

The technology of biomass air gasification seems to have a feasible application and has been developed actively for industrial applications. However, this technology produces a gas with a low heating value (4–6 MJ/m<sup>3</sup>) and an 8–14 vol% H<sub>2</sub> content [37]. Biomass oxygen-rich air gasification is one effective way of producing MHV gas, but it needs a large investment for oxygen production equipment and this disadvantage impedes its popularization.

Extensive experimental studies reported in the literature [38–41] show that fluidized bed, steam gasification processes (with or without O<sub>2</sub> added) are also capable of producing a middle heating value (10–16 MJ/Nm<sup>3</sup>) gas with a 30–60 vol% H<sub>2</sub> content. However, this technology requires that the temperature of steam be over 700 °C, which demands additional cost for steam generator of good performance [35,42]. Under this background, the technology of biomass air gasification with low-temperature steam is an attractive process. Since the steam gasification reactions are endothermic as a whole, the process must be supplied with energy. This can be done by partial combustion of biomass within the gasifier using a hypostoichiometric amount of air. A good agreement between the model predictions [43–46] and experimental data were obtained under the same operating conditions.

The basic reactions taking place during air/steam gasification are summarized in Table 3. The formula CH<sub>1.3</sub>O<sub>0.86</sub> was calculated from the ultimate analysis of various agricultural residues and average values of C, H, O content has been used [28,29].

Steam gasification of *Cynara Cardunculus* L. was carried out in a series of experiments in order to characterize the gas phase with a view to its energy use, analyzing the influence of temperature, particle size and water partial pressure [26]. Within the range of variables studied, the particle size had no effect on the overall process. Temperature and water partial pressure exerted positive effects on the main parameters of the process, increasing the reaction rate, the gas yield and production.

Steam gasification of three types of forestry biomass (pinus pinaster, eucalyptus, holm-oak) was studied in an atmospheric fluidized bed [47]. The gasifier was operated over a

Table 3  
Basic reactions during air and/or steam gasification

$2C + O_2 \leftrightarrow 2CO + 246.4 \text{ KJ}$	R-1
$C + O_2 \leftrightarrow CO_2 + 408.8 \text{ KJ}$	R-2
$CH_4 + H_2O \leftrightarrow CO + 3H_2 - 206 \text{ KJ}$	R-3
$CH_4 + 2H_2O \leftrightarrow CO_2 + 4H_2 - 165 \text{ KJ}$	R-4
$C + H_2O \leftrightarrow CO + H_2 - 131 \text{ KJ}$	R-5
$C + CO_2 \leftrightarrow 2CO - 172 \text{ KJ}$	R-6
$CH_{1.3}O_{0.89} + 0.88O_2 \leftrightarrow CO_2 + 0.65H_2O$	R-7
$CH_{1.3}O_{0.89} + 1.11H_2O \leftrightarrow CO_2 + 1.76H_2$	R-8
Agro residues	CH <sub>0.13</sub> O <sub>0.89</sub>

temperature range of 700–900 °C while varying a steam/biomass ratio from 0.4 to 0.85 w/w. The results obtained seemed to suggest that the operating conditions were optimized for a gasification temperature around 830 °C and a steam/biomass ratio of 0.6–0.7 w/w, because a gas richer in hydrogen and poorer in hydrocarbons and tars was produced. These conditions also favoured greater energy and carbon conversions, as well as the gas yield. The results reported come to an agreement with other results reported [48–50]. As biomass wastes usually have a problem of availability because of seasonal variations, this work analyzed the possibility of replacing one biomass species with another, without altering the gas quality obtained.

Synthetic gas with a high  $H_2/CO$  can be used for the production of pure hydrogen for fuel cell applications. Besides the high level of  $H_2/CO$  during commercial steam gasification, this ratio is increased during the water-gas shift reaction [ $C + H_2O \rightarrow CO + H_2$ ] for the removal of CO.

The steam to biomass ratio (S/B) can be altered either by changing the biomass feed rate keeping the steam flow rate constant or by changing the steam flow rate and keeping the biomass feed rate constant. A constant steam flow rate ensures constant residence time during the experimental procedure. The  $H_2$  concentration reached a maximum for (S/B) ranging between 0.6 and 0.7 [49,50]. For S/B ratios lower than 0.6 w/w, the results indicate [47,49,50] that there was not enough steam to react with all the biomass fed to the gasifier, keeping the water-gas shift reaction incomplete, resulting in a decrease in CO and hydrocarbon concentrations and in an increase of  $H_2$  concentration, which reached its maximum to an S/B ratio of 0.6–0.7. To these optimum S/B ratio values, the influencing reaction reach a state of equilibrium and, therefore,  $H_2$  reached its highest values.

Table 4 provides an overview of typical biomass gasification gas compositions from different gasifiers.

Table 4  
Typical biomass gasification gas compositions (mol.%)

Material	Medium	$T$ (°C)	$H_2$	$O_2$	$CH_4 + C_2H_x$	CO	$CO_2$	Ref.
Pine sawdust	Air	800	32.22	0.57	8.34	42.96	15.91	[46]
Crushed almond shells	Steam	820	47.5	—	6.2	32	14.3	[41]
Pine	Steam	800	34.4	—	12.15	40.3	13.15	[47]
Helm oak	Steam	800	42.13	—	8.92	29.75	19.2	[47]
Wheat straw	Air/Steam	697	20.96	0.33	22.15	35.6	20.96	[45]
Wheat straw	Air/Steam	660	18.7	0.864	21.336	27.4	31.7	[45]
Wheat straw	Air/Steam	609	21.1	2.16	22.27	23.84	30.63	[45]
Wheat straw	Air/Steam	766	18.27	11.33	19.82	33.33	17.25	[45]
Wheat straw	Air/Steam	740	18.46	6.45	18.79	26.57	29.73	[45]
Wheat straw	Air/Steam	672	21.45	8.3	19.18	20.1	30.97	[45]
Wheat straw	Air/Steam	816	20.8	3.03	21.43	33.33	21.41	[45]
Wheat straw	Air/Steam	792	19.06	7.75	18.27	25.04	29.88	[45]
Wheat straw	Air/Steam	719	21.07	3.58	17.66	18.83	38.86	[45]
Pinewood chips	Air	780–830	22	—	15.31	33.36	29.33	[40]
Cynara cardunculus L	Steam	650	52.1	—	3.51	17.9	25.4	[26]
Cynara cardunculus L	Steam	700	58.7	—	3.8	17.1	20.3	[26]
Cynara cardunculus L	Steam	750	60.0	—	3.7	18.3	18.1	[26]
Cynara cardunculus L	Steam	800	60.4	—	3.9	19.0	16.6	[26]



### 3. Fuel cells

Fuel cells are electrochemical devices that directly convert the chemical energy of a fuel to electricity, water vapor and surplus heat. Due to the direct conversion of chemical to electrical energy, fuel cells have a minimum environmental intrusion and the potential for high electrical efficiencies (35–55%), significantly higher than that of conventional power-generation systems, which are Carnot limited and lose efficiency because of thermodynamic and mechanical limitations in the system [1–4]. A single fuel cell consists of three parts: the anode, the cathode, an electrically insulating electrolyte or membrane separating the two electrodes. At the anode (negative electrode), fuel gas ( $\text{H}_2$ ,  $\text{CO}$ ,  $\text{CH}_4$ ) is fed and then diffuses towards the anode/electrolyte boundary, while an oxidant (air or oxygen) is fed continuously to the cathode (positive electrode). In the three-phase boundary (TPB) where anode, electrolyte and fuel gas coexist, the fuel components are oxidized liberating electrons as a result. Since the electrolyte is not electron conducting, electrons travel through an external circuit to the cathode, where they are accepted by oxygen atoms.

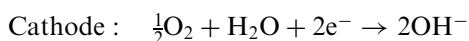
Hydrogen is the most commonly used fuel in the fuel cell technology, but natural gas, biomass gasification synthesis gas, petroleum-based fuel can also be used. The hydrogen electrochemical reaction used to produce electricity in a fuel cell produces water as the only “waste”. This chemical energy then can be converted to electricity through an electrochemical reaction that involves the oxidation of hydrogen with oxygen ions transferred from the electrolyte (anode side), obtained from the reduction of oxygen at the cathode side. The overall electrochemical reaction produces electrons and water as a waste product.

#### 3.1. Fuel cell types

Fuel cells are classified according to the type of electrolyte used in the cell and the operating conditions of the unit, among which temperature is the most important one. Low-temperature fuel cells operate below 200 °C and high-temperature fuel cells operate in the range 200–1200 °C.

##### 3.1.1. Alkaline fuel cells

In alkaline fuel cells (AFC), the electrolyte is a concentrated KOH solution. For low temperature (60–90 °C), the KOH concentration is 35–50 wt%. To achieve higher efficiency and optimum operation, the temperature was increased to 260 °C, using an 80–85 wt% KOH solution and an operating pressure of 4–6 atm, which prevents the electrolyte solution from boiling [1–4]. Pure  $\text{H}_2$  and  $\text{O}_2$  are input as the fuel and oxidizer in an AFC. The mobile charge carriers are the  $\text{OH}^-$  ions in the alkaline solution transferred from the cathode, where reduction of  $\text{O}_2$  occurs, to the anode, where oxidation of  $\text{H}_2$  occurs. The gas-diffusion electrodes are constructed of porous carbon and are doped with platinum (Pt) catalysts to catalyze the oxidation and reduction reactions, overcoming the problem of slow reaction rates [1,2]. The operation of AFC is defined by the following reactions [3]:



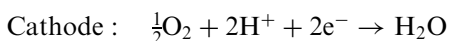
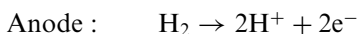


AFC have the highest electrical efficiency of all fuel cell systems (~60% LHV), but are reported to be extremely sensitive to impurities. The presence of  $N_2$  and impurities in the gas streams reduce the fuel cell efficiency. The presence of  $CO_2$  reduces the ionic conductivity of the electrolyte and inhibits gas diffusion through the carbon electrodes, due to the formation of  $K_2CO_3$  produced by the reaction of carbon dioxide present in air with the electrode, causing the above blocking effect and, therefore, reducing effectiveness and the reaction rate at the anode [1,3]. In order to overcome this poisoning effect of  $CO_2$  it is necessary to purify both  $H_2$  and  $O_2$  used in the cell, adding a high additional cost.

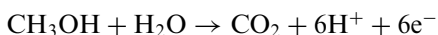
### 3.1.2. Polymer electrolyte membrane fuel cells

In polymer electrolyte membrane fuel cells (PEMFC), also referred to as proton-exchange membrane fuel cells, the electrolyte is an ion exchange membrane, which is an excellent proton conductor. The membrane material is a fluorinated sulfonic acid polymer [1,2]. The acid molecules are immobile in the matrix, while the protons associated with these acid groups are free to migrate through the membrane from the anode to cathode where water is produced.

Since water is the only liquid present in the unit, corrosion problems are minimal. Water management in the membrane is critical for efficient performance, since the fuel cell must operate under conditions where the byproduct water does not evaporate at a rate higher than it is produced, in order to maintain the optimum level of humidity. Because of the limitation on the operating temperature imposed by the polymer (50–200 °C), the reaction rates are low and the addition of platinum catalyst in the anode is incorporated in order to catalyze the reaction. The operation of PEMFC is defined by the following reactions [3]:



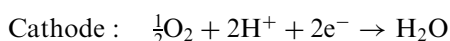
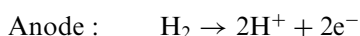
PEMFC are very sensible to impurities, especially to CO, thus high-purity hydrogen is required as a fuel. Carbon monoxide, even in very low concentrations, reduces the overall performance of the fuel cell, due to CO adsorption on the anode Pt catalyst. The Pt–CO bond is stronger than the Pt–H bond blocking the cell reactions. Carbon dioxide can also affect the cell's performance since it may be converted to carbon monoxide via the water–gas shift reaction [1,2]. On the other hand, the low operating temperature allows a better handling of the stack materials and sealant problems are easier to overcome compared to high-temperature fuel cells. Methanol can also be used as a fuel, which is a promising fuel in terms of availability and cost compared to hydrogen. Even though methanol reacts slowly following reaction 5.5, leading to a high activation polarization, the high-density power, availability, minimum storage problems and easy to overcome safety issues make this technology an attractive alternative to the use of hydrogen in PEMFC [1,4].



### 3.1.3. Phosphoric acid fuel cells

Phosphoric acid fuel cells (PAFC) operate at medium temperatures (up to 200 °C) and are regarded as the most mature and are close to commercialization fuel cell technology [2,4].

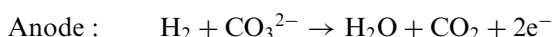
In PAFC, the electrolyte is 100% concentrated phosphoric acid, which is immobilized in a silicon carbide-poly(tetrafluoroethylene) (SiC-PTFE) matrix, acting also as a proton-conducting material. The electrolyte must be kept in a temperature above 42 °C to avoid freezing. The electrodes are made of Pt dispersed on carbon bonded with PTFE (35–50 wt%). PAFC are tolerant to CO<sub>2</sub>, allowing air to be used as the oxidant, and have demonstrated high thermal, chemical and electrochemical stability [1,2,4]. The operation of PAFC is defined by the following reactions [3]:



The water produced in the cathode is removed with the excess O<sub>2</sub> and the N<sub>2</sub>. Aside from the CO produced during hydrocarbon reforming, which PAFC can tolerate to a concentration up to 1 vol%, the concentration of other impurities must be low. Sulfur gases (mainly H<sub>2</sub>S) that originate from the fuel gas can poison the anode by blocking active sites for H<sub>2</sub> oxidation on the Pt surface.

#### 3.1.4. Molten carbonate fuel cells

Molten carbonate fuel cells (MCFC) are high-temperature fuel cells where the electrolyte is alkali carbonates (Li, Na, K) stabilized in a LiAlO<sub>2</sub> ceramic matrix. In the high operating temperatures (600–700 °C), these carbonates form molten salts. Electrons are conducted from the anode through an external circuit to the cathode and a negative charge is conducted from the cathode through the electrolyte by CO<sub>3</sub><sup>2-</sup> ions to the anode. Water is produced at the anode and removed with CO<sub>2</sub>. CO<sub>2</sub> needs to be recycled back to the fuel cell anode to maintain the electrolyte composition, a process that makes MCFC more complicated than other fuel cell types in order to provide the appropriate fuel distribution [1]. The operation of MCFC is defined by the following reactions [3]:



The above electrochemical reactions are unique in the sense that carbon dioxide is consumed in the cathode and produced in the anode. The high operating temperatures provide the potential for high overall system efficiencies, especially if the waste heat of the process is utilized in the fuel-reforming step or for cogeneration and also widen the fuel flexibility since a variety of hydrocarbons (natural gas, alcohols, landfill gas, synthesis gas from coke, coal and biomass) can be reformed to generate hydrogen for the fuel cell. The carbon monoxide present in biomass and/or coal gasification producer gas and reformed hydrocarbons is not used directly in the MCFC, but via the water gas-shift reaction in order to produce additional hydrogen. The anode contains Ni doped with 10% Cr to promote sintering. The presence of Ni in the anode and the high operating temperatures make MCFC suitable for internal CH<sub>4</sub> reforming, a process that increases the system's overall efficiency, induces unwanted temperature gradients inside the fuel cell that may cause material problems and also reduces cost.

### 3.1.5. Solid oxide fuel cells

SOFC operate at temperatures between 600 and 1000 °C. The electrolyte material in an SOFC is yttrium-stabilized zirconia (YSZ), a solid with a stable cubic structure and high oxide conductivity at SOFC operating temperatures. The anode material is a Ni cermet (ceramic and metal composite) [1–4]. It contains metallic Ni for catalytic activity in an YSZ support, which adds mechanical, thermal and chemical stability and thermal. The cathode consists of mixed oxide with a perovskite crystalline structure, typically strontium-doped lanthanum manganite (LSM). The high operating temperatures allow higher fuel flexibility, because in the presence of enough vapor and oxygen complete oxidation is achieved, without catalytic materials being present. The operation of an SOFC fuelled with biomass gasification gas is defined by the following reactions [2]:

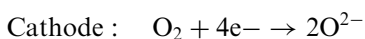
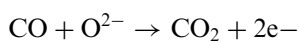
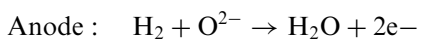


Table 5 summarizes the main operating features of the fuel cell types discussed above.

The advantages of operating at high temperature is that the heat evolved in the fuel cell can be used for cogeneration or bottoming cycles, as part of a highly efficient integral-conversion system. SOFC are being investigated on integrated systems such as SOFC-gas turbine [11,51–56] and thermal integration with gasification systems [15,20,57–63]. Furthermore, the waste heat can be used for providing the energy necessary in the reforming process, either external or internal [21,64,65]. Hopefully, sufficient research, to form a base and orientate the proposed project, has been devoted to SOFC operation on synthesis gas. Numerous studies report performance characteristics on the steam dilution of  $\text{H}_2$ , while some of them also examine the effect of fuel composition [66]. Furthermore, over Ni/YSZ anodes, Jiang reported a 60% drop of the current density when CO was diluted to 50% by  $\text{CO}_2$  [67]. Generally,  $\text{H}_2$  electro-oxidation is 2–3 times faster than

Table 5  
Fuel cell types and main operating characteristics

Fuel cell type	Electrolyte	Charge carrier	Anode reaction	Cathode reaction	Operating temperature	Electric efficiency (%)
AFC	KOH	$\text{OH}^-$	$\text{H}_2 + 2\text{OH}^- \rightarrow 2\text{H}_2\text{O} + 2\text{e}^-$	$\frac{1}{2} \text{O}_2 + \text{H}_2\text{O} + 2\text{e}^- \rightarrow 2\text{OH}^-$	60–120	35–55
PEMFC	Solid Polymer	$\text{H}^+$	$\text{H}_2 \rightarrow 2\text{H}^+ + 2\text{e}^-$	$\frac{1}{2} \text{O}_2 + 2\text{H}^+ + 2\text{e}^- \rightarrow \text{H}_2\text{O}$	50–100	35–45
PAFC	Phosphoric Acid	$\text{H}^+$	$\text{H}_2 \rightarrow 2\text{H}^+ + 2\text{e}^-$	$\frac{1}{2} \text{O}_2 + 2\text{H}^+ + 2\text{e}^- \rightarrow \text{H}_2\text{O}$	220	40
MCFC	Lithium and potassium carbonate	$\text{CO}_3^{2-}$	$\text{H}_2 + \text{CO}_3^{2-} \rightarrow \text{H}_2\text{O} + \text{CO}_2 + 2\text{e}^-$	$\frac{1}{2} \text{O}_2 + \text{CO}_2 + 2\text{e}^- \rightarrow \text{CO}_3^{2-}$	650	> 50
SOFC	Solid oxide (YSZ)	$\text{O}^{2-}$	$\text{H}_2 + \text{O}^{2-} \rightarrow \text{H}_2\text{O} + 2\text{e}^-$	$\text{H}_2 + \text{O}^{2-} \rightarrow \text{H}_2\text{O} + 2\text{e}^-$	1000	> 50

CO's [66], due to the insufficient spillover of the latest to the TPB of the electrode-electrolyte interface [67]. This results up to 5 times lower CO contribution to the cell's power output, compared to  $H_2$ , over the most commonly used Ni/YSZ anodes [68]. While CO is a poor fuel for Ni-based anodes, it can be used to produce additional  $H_2$ , through the gas shift reaction, which is catalysed by Ni containing anodes. Apart from  $H_2O$  produced by the electro-oxidation of  $H_2$ , additional steam can be introduced to the cell, to improve performance, a case that coincides with internal reforming SOFCs [69]. In order to enhance SOFC performance and prevent carbon deactivation, several composite anodes have been tested [70]. Exceptional enhancement of CO contribution to the overall power density was observed over Cu/CeO<sub>2</sub>/YSZ anodes [67], which are often tested for the direct C<sub>x</sub>H<sub>y</sub> oxidation in SOFCs, and exhibit high resistance to coking [71]. Cobalt incorporation to these catalysts further improves their performance [72], and leads to CO power densities higher than even those of  $H_2$  [67]. This was attributed to the expansion of electrochemically active zone of the anode, to the extended surface of O<sup>2-</sup> conducting CeO<sub>2</sub> [67]. Ni, Cu, Co, Fe, as well as Pt- and Rh-active phases, will be (solely or combined) incorporated with CeO<sub>2</sub>/YSZ substrates in order to develop state-of-the-art composite anodes, for the optimum CO contribution to the overall cell performance (since CO is a major component in various biogas compositions). Biogas-fuelled SOFCs seem to fit this tool extraordinarily, since operating voltage controls fuel conversion. Thus, by externally affecting SOFC's voltage, diluted fuel utilization is expected to be enhanced. In any case, biogas will be fed to the experimental SOFC modules, either pre-reformed or with additional steam, for internal reforming (steam or dry) operation of the SOFC. Furthermore, state-of-the-art composite cathodes will also be studied in order to minimize cathodic overpotential losses and to explore the possibility of operating SOFC under O<sub>2</sub>-depleting cathodic conditions (i.e. to decrease O<sub>2</sub> concentration at the exit of the cathode, to low values). This possibility can potentially increase the thermal efficiency of the cell, eliminate air-preheating requirements (since decreased air excess will be fed to the cell) and provide a high-temperature, O<sub>2</sub>-lean medium to be circulated to the pyrolyzer of the integrated process.

The latest option incorporates the inherent ability of SOFC devices to separate O<sub>2</sub> from N<sub>2</sub>, and may lead to a significant reduction of the costs related to N<sub>2</sub>/O<sub>2</sub> separation for biomass pyrolysis. Of course, these potential advantages have to be counterbalanced to an inevitable decrease of SOFC's electrical efficiency and pyrolysis yield, the latest due to the presence of O<sub>2</sub> in cathodes exhaust gas, even at low concentrations. State-of-the-art cathode composites primarily include mixed conducting materials, such as the already established LaSrMn perovskites [73], CeO<sub>2</sub> [74] and the more-effective LaSrCoFe perovskites [74], quite often in YSZ or CGO cermets [73].

Despite the benefits of fuel cells, their potential to become a viable option depends foremost on the capital cost of the system. Fuel cell needs to be cost-competitive compared to conventional power-generation systems. Table 6 summarizes the capital costs of several power-generation systems. Table 6 states that, with the exception of solar PV, fuel cell capital costs are higher than other conventional or renewable power-generation systems. Given the high capital cost, which is partly balanced by the high overall system efficiencies, fuel choice is another important factor.

The main advantages of fuel cells are [1–4] high efficiency, size flexibility, high reliability, emissions, ease of installation, silent operation and fuel flexibility.

The main disadvantages of fuel cells are [1–4] cost, size and weight, start-up time, durability and fuel availability.

Table 6  
Capital costs of power generation systems

Technology	Typical installed capital cost (\$/KW)
Gas turbine	700–900
Microturbine	700–1300
Steam turbine	800–1000
Wind turbine	800–1250
Natural gas engine	800–1500
Fuel cell	> 2800
Solar photovoltaic	> 5000

Since the fuel gas quality and the fuel processing are increasingly important as the fuel cell operating temperature decreases, molten carbonate and SOFC have the higher fuel flexibility, the lowest fuel-quality demands and furthermore carbon monoxide does not cause poisoning since it can be directly electrochemically oxidized in MCFC and SOFC. These high operating temperatures of MCFC and SOFC enable the internal reforming of light hydrocarbons to hydrogen and carbon monoxide and the use of a wide range of fuels. As mentioned above, one important feature of SOFC is that all system components are solid allowing several stack configurations, a feature not available in MCFC where there are limitations constrained by the fact that the electrolyte cannot be oriented in any position. In addition, the required CO<sub>2</sub> supply to the cathode of MCFC is a disadvantage associated with system complexity.

Biomass gasification, which is investigated in the present study, is normally carried out to temperatures around 900 °C, which is in the SOFC-operating temperature interval, making thermal integration of biomass gasification with SOFC viable and theoretically easy to accomplish. SOFC seems to be the most promising fuel cell technology of biomass gasifier producer gases.

SOFCs, because of their high operating temperatures, do not require pure hydrogen as fuel, exhibiting a high fuel flexibility, which is a major advantage concerning the high cost of hydrogen production. The operation of SOFC on various fuels such as natural gas, biogas, biomass gasification gas, coal gasification gas has been an active area of research. The most common fuel is natural gas, which is low cost, clean, abundant and available and with a well-developed supply chain worldwide.

### 3.2. Thermodynamic analysis

SOFCs operate at high temperature (600–1200 °C), which makes possible the use of a variety of fuels (hydrocarbons), cogeneration and bottoming cycles. In a thermally integrated biomass SOFC-gasification system (BG-SOFC), the producer gas (a mixture of hydrogen, methane, carbon monoxide, carbon dioxide, small amounts of tars <1% and steam) from the gasifier will be fed into the SOFC, and the hot effluent gases from the anode and cathode will be re-injected into the gasifier (at different gasification zones), maintaining the reactor temperature. At high temperatures, methane will be internally reformed in the SOFC and carbon monoxide will be converted to hydrogen (assuming that the water-gas shift reaction will always be at equilibrium) [65].

Conversion efficiencies are expected up to 45% (BG-SOFC) based on modeling analyses [57]. The accurate prediction of SOFC operating conditions is important for attaining high efficiencies and successfully integrating both systems (BG-SOFC). The spectrum of possible operating conditions can be determined based on the performance characteristics of the fuel cell. These characteristics will allow us to determine a set of operating conditions (temperature, pressure, inlet compositions) for optimal performance.

The fuel cell performance is subject to the second law of thermodynamics, so that losses in the system are inevitable. For a fuel cell, the main sources of irreversibility are ionic resistance through the electrolyte and electronic resistance on the electrodes and interconnects, activation energy, the diffusion of gases to the reaction sites. These losses can be determined numerically or experimentally. However, numerical models are preferred for economical reasons and because sensitivity to different parameters can be investigated with the same model. There are, in general, three types of numerical models used for determining the polarization terms in SOFCs: micro-level models [75–79], macro-level models [80–83] and semiempirical models [84–86]. Results presented in this chapter are based on a macrolevel model. This model is based on the assumption that the reactions occur at the electrode–electrolyte interface, and, therefore, no analysis at the microscopic level is required. This assumption is valid for pure electronic conductors but is unrealistic for cermet-type anodes (i.e., Ni-YSZ), because of the intermixing in the electrode–electrolyte interface. However, based on the cermet-modeling results by Chan and Xia [87], it can be argued that most of the polarization contribution occurs at the interface, especially for anode-supported cells with thick anodes (600  $\mu\text{m}$ ).

The integrated process of biomass gasifier and an SOFC was studied in terms of thermodynamics. Since both processes perform around 1000 °C, heat integration is one of the benefits of the proposed scheme, according to which the cathode outlet of the cell can be directly fed to the gasifier. The thermodynamic analysis was based on the regulation of oxygen consumption in the cell, so that the depleted air fed to the gasifier led to the minimization of the total combustion reactions in the latest. According to the assumption that the hydrogen content of the biomass feedstock is totally converted to hydrocarbons (methane for simplicity), during gasification under oxygen lean conditions, while the remaining carbon is only partially oxidized to carbon monoxide, as well as that both hydrogen and carbon monoxide were both oxidized in the SOFC, at the appropriate extent, the energy balance revealed that the process can be auto-thermal. Furthermore, and due to the utilization of the hydrogen content of steam utilized in the reforming stage, the overall efficiencies to electrical power could reach very high levels [88].

### 3.2.1. Chemical thermodynamics

Using the first and second laws of thermodynamics, a simple and fundamental description of the ideal reversible fuel cell can be determined. The first law of thermodynamics states that the energy of a system is conserved. Energy cannot be lost or generated, but can only be converted from one form to another. For a control volume, which is an open system that involves flow of mass across its boundaries, the first law of thermodynamics is defined by the following equation [1]:

$$\delta Q - \delta W = dE. \quad (3.1)$$

Eq. (3.1) uses the sign convention of positive for input and negative for output:  $Q$  is the heat entering the system,  $-W$  the work performed by the system,  $E$  the total energy of the

system. A change in heat or work is expressed by an inexact differential,  $\delta$ , because the values are dependent on path and called path functions. Energy is a property and is a point function, dependent only on the initial and final states. When Eq. (3.1) is integrated, the first law of thermodynamics is expressed by the following relation [1]:

$$Q - W = \Delta E = \Delta U + \Delta KE + \Delta PE + \Delta PV, \quad (3.2)$$

where  $\Delta U$  is the internal energy,  $\Delta KE$  the kinetic energy,  $\Delta PE$  the potential energy,  $\Delta PV$  is the work that is exerted on the fluid to keep it flowing.

For a stationary control volume under steady state (flow) conditions, the kinetic and potential energies are constant with time, thus  $\Delta KE = \Delta PE = 0$ . The first law of thermodynamic is written:

$$Q - W = \Delta U + \Delta PV. \quad (3.3)$$

The property enthalpy ( $H$ ) is defined and accounts for the flow work:

$$H = U + PV. \quad (3.4)$$

Thus Eq. (3.3) becomes:

$$Q - W = \Delta U + \Delta PV \Rightarrow \Delta H = Q - W. \quad (3.5)$$

The second law of thermodynamics defines the property entropy, which can be used as an indication of the disorder of the system. A process that does not generate entropy is called reversible process and can be performed and then returned to its initial state. Therefore in a reversible process, no net exchange of heat or work occurs in either the system or the surrounding environment [1,2]. Entropy is based on this reversible heat transfer, and as a property is expressed by the following equation:

$$dS = \left( \frac{\delta Q}{T} \right)_{\text{rev}} \Rightarrow \Delta S = S_2 - S_1 = \int_1^2 \left( \frac{\delta Q}{T} \right)_{\text{rev}}. \quad (3.6)$$

The reaction entropy  $\Delta S$  is a result of the reaction itself and must be compensated by the transport of the reversible heat  $Q_{\text{rev}}$  to the environment. Thus Eq. (3.6) becomes:

$$\Delta S = \frac{Q_{\text{rev}}}{T_O}. \quad (3.7)$$

Substituting Eq. (3.7) into Eq. (3.3)

$$\Delta ST_O + W_{\text{rev}} = \Delta H \Rightarrow W_{\text{rev}} = \Delta H - \Delta ST_O. \quad (3.8)$$

The Gibbs free energy ( $G$ ) is defined by the following equation:

$$G = H - TS. \quad (3.9)$$

Chemical reactions proceed in the direction that minimizes the Gibbs energy. Based on the definition of Gibbs energy, enthalpy  $H$  and Eq. (3.1) the following equation is derived:

$$\begin{aligned} G = H - TS &\Rightarrow dG = dH - d(TS) \Rightarrow dG = dH - T dS - S dT \Rightarrow dG \\ &= d(U + PV) - T dS - S dT \Rightarrow dG = dU + P dV + V dP - T dS - S dT. \end{aligned} \quad (3.10)$$

The term  $dU$  is replaced by the first law of thermodynamics as described by Eq. (3.1), resulting in a general expression for the change in Gibbs energy as applied to a closed,



stationary system ( $\Delta E = 0$ ; properties constant with time):

$$dG = \delta Q - \delta W + P dV + V dP - T dS - S dT. \quad (3.11)$$

For a reaction at constant temperature and pressure ( $V dP = S dT = 0$ ) and considering that fuel cell systems are restricted only to expansion-type work ( $\delta W = P dV$ ), Eq. (3.11) becomes:

$$dG = \delta Q - T dS. \quad (3.12)$$

Combining Eq. (3.12) and the second law of thermodynamics becomes as expressed by Eq. (3.7), using an inequality sign:

$$dS \geq \left( \frac{\delta Q}{T} \right)_{\text{rev,irrev}} \Rightarrow \delta Q - T dS \leq 0 \Rightarrow dG = \delta Q - T dS \leq 0. \quad (3.13)$$

In order to satisfy the second law of thermodynamics, a reaction at constant temperature and pressure should proceed in a direction of negative change in Gibbs energy reaches a minimum where  $dG = 0$ , and the reaction is at equilibrium.

The Gibbs free energy is a function of temperature and pressure as indicated by Eq. (3.11). For a to the point that reversible system where  $\delta Q - T dS = 0$  and considering that fuel cell systems are restricted only to expansion-type work ( $\delta W = P dV$ ), Eq. (3.11) becomes

$$dG = V dP - S dT. \quad (3.14)$$

The ideal gas equation is given by the following expression:

$$PV = nRT \Rightarrow V = \frac{nRT}{P}, \quad (3.15)$$

where  $n$  is the number of moles,  $R$  the molar gas constant and  $T$  the absolute temperature.

Considering an ideal gas at a constant temperature ( $dT = 0$ ), the Gibbs energy at a given pressure can be determined with respect to its value at a reference pressure from Eq. (3.14):

$$dG = V dP - S dT \Rightarrow dG = V dP \Rightarrow dG = nRT \frac{dP}{P} \Rightarrow \int_1^2 dG = \int_1^2 nRT \frac{dP}{P}. \quad (3.16)$$

Thus the effect of pressure on Gibbs energy at a constant temperature is given by the following expression:

$$\Delta G = G_2 - G_1 = nRT \ln \left( \frac{P_2}{P_1} \right) \Rightarrow G_2 = G_1 + nRT \ln \left( \frac{P_2}{P_1} \right). \quad (3.17)$$

The above Eq. (3.17) can be rewritten in molar quantity terms, assuming that state 1 is replaced by a standard reference state where  $G_1 = G^\circ$  and  $\alpha$  reference pressure  $P_1 = P^\circ$ :

$$G_2 = G^\circ + nRT \ln \left( \frac{P_2}{P^\circ} \right) \Rightarrow g = g^\circ + RT \ln \left( \frac{P_2}{P^\circ} \right) \Rightarrow g_i(T, P_i) = g_i^\circ(T) + RT \ln \left( \frac{P_i}{P^\circ} \right). \quad (3.18)$$

For a general reaction scheme, as shown below, in a constant temperature and pressure the reactants  $A$  and  $B$  form the products  $C$  and  $D$ :



where the capital letters indicate the chemical constituents and  $v_i$  the stoichiometric coefficients associated with the balanced reaction. Based on Eq. (3.17), the change in Gibbs energy is denoted as the difference between the products and reactants. Thus [1,2],

$$\begin{aligned} \Delta G &= v_C g_C + v_D g_D - v_A g_A - v_B g_B \Rightarrow \Delta G = v_C g_C^0 + v_D g_D^0 - v_A g_A^0 - v_B g_D^0 \\ &+ RT \left[ v_C \ln \left( \frac{P_C}{P^0} \right) + v_D \ln \left( \frac{P_D}{P^0} \right) - v_A \ln \left( \frac{P_A}{P^0} \right) - v_B \ln \left( \frac{P_B}{P^0} \right) \right]. \end{aligned} \quad (3.20)$$

The standard Gibbs energy terms can be expressed as the standard state Gibbs function ( $\Delta G^0$ ):

$$\Delta G = \Delta G^0 + RT \left[ v_C \ln \left( \frac{P_C}{P^0} \right) + v_D \ln \left( \frac{P_D}{P^0} \right) - v_A \ln \left( \frac{P_A}{P^0} \right) - v_B \ln \left( \frac{P_B}{P^0} \right) \right]. \quad (3.21)$$

Considering a reference pressure  $P^0 = 1$  atm Eq. (3.21) results in:

$$\Delta G = \Delta G^0 + RT \left[ \ln \left( \frac{P_C^{v_C} P_D^{v_D}}{P_A^{v_A} P_B^{v_B}} \right) \right]. \quad (3.22)$$

Chemical reactions satisfy the second law of thermodynamics and proceed in a direction of negative change in Gibbs energy and reach a minimum, where  $dG = 0$ , and the reaction is at equilibrium. The standard state Gibbs energy corresponds to the maximum work that can be drawn from the system that operates at constant conditions. Consequently, Eq. (3.22) results in:

$$\Delta G^0 = -RT \left[ \ln \left( \frac{P_C^{v_C} P_D^{v_D}}{P_A^{v_A} P_B^{v_B}} \right) \right] \Rightarrow \Delta G^0 = -RT \ln K_P. \quad (3.23)$$

Eq. (3.23) defines the equilibrium constant  $K_P$ , which can also be expressed in terms of mole fractions ( $p_i = x_i p$ ). Thus,

$$K_P = \frac{P_C^{v_C} P_D^{v_D}}{P_A^{v_A} P_B^{v_B}} \Rightarrow K_P = \frac{x_C^{v_C} x_D^{v_D}}{x_A^{v_A} x_B^{v_B}} (p)^{v_C + v_D - v_A - v_B}. \quad (3.24)$$

The maximum thermal efficiency that a heat engine reaches is given by the theoretical Carnot cycle, which is thermodynamically reversible and depends on the ration of the low ( $T_L$ ) and high ( $T_H$ ) temperature of the thermodynamic cycle. This theoretical efficiency is described by the following equation:

$$n_{\text{Carnot}} = 1 - \frac{T_L}{T_H}. \quad (3.25)$$

To reach the highest possible temperature leading to the highest efficiency, however, the fuel loses a portion of its chemical energy to irreversible processes that occur during combustion. Electrochemical cells, such as storage batteries and fuel cell, operate at constant temperatures with the products of the reaction leaving them at the same temperature as the reactants. Because of this isothermal reaction, more of the chemical energy of the reactants is converted to electrical energy instead of being consumed to raise the temperature of the products. As a result, the electrochemical conversion process is less

irreversible than the combustion reaction. The maximum work that an electrochemical cell can perform is associated with the change in Gibbs as expressed by Eq. (3.11) and the second law of thermodynamics for a reversible process ( $\delta Q = TdS$ ):

$$dG = -\delta W + PdV + VdP - SdT. \quad (3.26)$$

At constant temperature and pressure, Eq. (3.26) becomes:

$$dG = -\delta W + PdV \Rightarrow dG = -(\delta W - PdV). \quad (3.27)$$

Eq. (3.27) shows that the change in Gibbs energy of a chemical reaction is the non-expansion work the system can perform. This work is done by the movement of electrical charge through a voltage called the electrochemical work,  $W_{FC,rev}$ .

$$dG = -\delta W_{FC,rev} \Rightarrow \int dG = - \int \delta W_{FC,rev} \Rightarrow \Delta G = -W_{FC,rev}. \quad (3.28)$$

Assuming a reversible reaction, meaning that the Gibbs free energy is converted into electrical energy, the Gibbs energy can be used to find the open-circuit voltage of the fuel cell.

If we designate as  $(-e)$  as the charge on one electron, then the charge that is produced by the reaction is

$$I = -zNe = -zF, \quad (3.29)$$

where  $F$  is the Faraday constant ( $F = 9.6485 \times 10^4 \text{ C/mol}$ ), which is the charge on one mole of electrons, and  $N$  is Avogadro's number ( $N = 6.023 \times 10^{23}$ ). The electrical work done by the fuel cell operates at a voltage  $E$ :

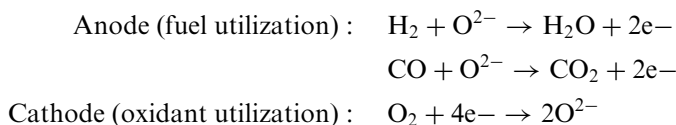
$$W_{FC,rev} = EI = -z(Ne)E = -zFE. \quad (3.30)$$

Substituting Eq. (3.30) into Eq. (3.28) and considering Eq. (3.22) results in the following off-equilibrium condition Nernst's equation, which defines the reversible open-circuit voltage or electromotive force (EMF):

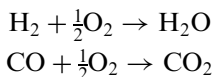
$$\begin{aligned} \Delta G = -zFE \Rightarrow \Delta G^0 + RT \left[ \ln \left( \frac{P_C^{v_C} P_D^{v_D}}{P_A^{v_A} P_B^{v_B}} \right) \right] &= -zFE \Rightarrow E = - \left( \frac{\Delta G^0}{zF} \right) - \frac{RT}{zF} \left[ \ln \left( \frac{P_C^{v_C} P_D^{v_D}}{P_A^{v_A} P_B^{v_B}} \right) \right] \\ \Rightarrow E = E^0 - \frac{RT}{zF} \left[ \ln \left( \frac{P_C^{v_C} P_D^{v_D}}{P_A^{v_A} P_B^{v_B}} \right) \right] &= E^0 - \frac{RT}{zF} \left[ \ln \prod_i \left( \frac{P_i}{P^0} \right)^{v_i} \right], \end{aligned} \quad (3.31)$$

where  $E^0 = -(\Delta G^0/zF)$  is the maximum voltage obtained from the fuel cell, called maximum open-circuit voltage.

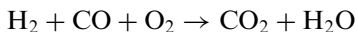
As mentioned above, the main reactions of SOFC using biomass gasification gas as a fuel are the following:



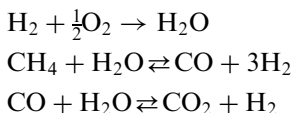
Thus, the overall cell reactions are



or:



The above reaction scheme states that  $\text{H}_2$  and  $\text{CO}$  are the two electrochemically active fuel species. Based on the assumption that the electrochemical oxidation of  $\text{CO}$  and  $\text{CH}_4$  is slower than the water-gas shift and reforming reaction producing  $\text{H}_2$ , the above-described model can be used for hydrogen, methane and carbon monoxide with ( $\text{H}_2$  being the only electrochemical active fuel specie) the reforming reaction for methane and the water gas shift reaction for carbon monoxide, according to the following reactions [20,57]:



Following the above assumptions, Eq. (3.31) becomes:

$$E = -\left(\frac{\Delta G^\circ}{2F}\right) - \frac{RT}{2F} \left[ \ln \left( \frac{P_{\text{H}_2\text{O}}}{P_{\text{H}_2} P_{\text{O}_2}^{1/2}} \right) \right] \Rightarrow E = E^\circ - \frac{RT}{2F} \left[ \ln \left( \frac{P_{\text{H}_2\text{O}}}{P_{\text{H}_2} P_{\text{O}_2}^{1/2}} \right) \right]. \quad (3.32)$$

The open-circuit voltage [ $E^\circ$ ] is 1.229 V considering liquid water as product, and 1.185 considering a gaseous water product. The difference between the two calculated values represents the latent heat of vaporization of water at standard conditions. Eq. (3.32) is a measure of the driving force for the generation of current in the cell and it is dependent on cell temperature, hydrogen and water concentration in the fuel gas (anode) and oxygen in the cathode. The effect of the logarithmic term  $\ln(P_{\text{H}_2\text{O}}/P_{\text{H}_2} P_{\text{O}_2}^{1/2})$  in the partial pressures is to gauge the change in potential due to changes in reactant and/or product concentration.

The Nernst equation represents an ideal operation of the fuel cell. The actual cell potential is decreased because of irreversible losses. These losses called polarizations or overpotentials ( $\eta$ ) originate from three sources: activation polarization ( $\eta_A$ ), ohmic polarization ( $\eta_\Omega$ ) and concentration polarization ( $\eta_D$ ). These polarizations result in an actual cell voltage less than the ideal potential given by Eq. (3.32), [20,55–59,89,90].

As stated above, a single SOFC is made of three parts: anode, electrolyte and cathode. The electrolyte is made dense and gas tight, thus separating the fuel and air streams to the anode and cathode. The cathode and anode are made porous to facilitate diffusion of the gaseous reactants and reaction products through the electrodes. Apart from separating the gas streams, the purpose of the electrolyte is to conduct oxygen ions from the cathode to the anode. At the TPB, where cathode material, electrolyte material and gaseous oxygen meet, oxygen molecules are reduced to oxygen ions by accepting electrons from the cathode material [1,2]. The oxygen ions are transported through the electrolyte to the three-phase boundary on the anode side. Here, in the region where anode material, electrolyte material and fuel meet, the oxygen ions react with  $\text{H}_2$  and  $\text{CO}$  to produce  $\text{H}_2\text{O}$  and  $\text{CO}_2$ , respectively. The electrons thus liberated are conducted through the external circuit to the cathode thus closing the complete circuit. By including a load in the external

circuit, electrical power is produced. As mentioned, the operating voltage of the SOFC is governed by Nerst's Eq. (3.31). As current passes through the fuel cell,  $H_2$  and CO are electrochemically oxidized, liberating electrons. Considering for purposes of simplicity that hydrogen is the only electrochemically active fuel (for the case of biomass gasification derived gas), it is clear that the number of electrons liberated at the anode is twice the number of hydrogen molecules consumed, so the molar flow of electrons is twice the molar flow of hydrogen.

Fuel utilization is expressed with the above assumption in terms of molar flow of hydrogen entering and leaving the fuel cell. Thus [1,2]:

$$U_f = 1 - \frac{m_{H_2,out}}{m_{H_2,in}}. \quad (3.33)$$

At low fuel utilization when the fuel flow is large compared to the current drawn, the fuel gas is practically unchanged leaving the cell. In this case the Nerst potential is even over the entire fuel cell and can be calculated based on the inlet gas composition. As fuel utilization increases, the gas composition is changed by the production of  $H_2O$  and  $CO_2$ . The cell voltage decreases as the increasingly diluted gas travels over the cell area.

In our on-going project, from the thermodynamic analysis of the integrated process of biomass gasification of the solid oxide fuel cell, it becomes obvious that the overall heat generated can cover the heat demands of the reforming procedure and furthermore allow the production of extra electrical power at a conventional heat engine. The extra hydrogen introduced in the process, during the reforming stage, can enhance the electrical efficiency. Of course one must take into account the thermal losses in the several stages of the overall process, which were neglected in the present study [88].

### 3.2.2. Steam reforming

Steam reforming is a common method used in most commercial SOFC systems for producing hydrogen from light hydrocarbon (natural gas, landfill gas, biomass gasification gas). Fuel is mixed with superheated steam at temperatures up to  $1000^\circ C$ , under pressure and in the presence of nickel-based catalysts. Carbon in the fuel is oxidized producing carbon monoxide while hydrogen is released.

The reforming reaction is described by the following general scheme:



The above general scheme for the case of methane becomes:



Additional hydrogen can be produced via the shift reaction:



Three different reforming configurations are available: external reforming, indirect internal reforming and direct internal reforming.

External reforming requires an external heat source such as burner of hot waste gas. In an SOFC, the hydrocarbon fuel is catalytically converted (internally reformed), generally to hydrogen and carbon monoxide (synthesis gas), together with some carbon dioxide, within the cell stack, and the carbon monoxide and hydrogen are then electrochemically oxidized to carbon dioxide and water at the anode, with production of electrical power and

high-grade heat. Internal reforming capitalizes on the heat release in the fuel oxidation process. Internal reforming of the fuel can either be achieved either indirectly using a separate fuel reforming catalyst within the SOFC stack or directly on the anode.

Internal reforming of the fuel within the SOFC stack is preferred, since this increases the operational efficiency to well above that of low-temperature fuel cells and reduces the complexity of the system, hence reducing cost [91]. However, there are several major problems concerning internal reforming in a solid oxide fuel cell, which can lead to deactivation and the major loss is system efficiency, such as carbon deposition due to hydrocarbon pyrolysis [1–4,91]. The risk for carbon formation through side reactions such as methane cracking, Boudourd coking and CO reduction is reduced by increasing the steam-to-carbon ratio (S/C) of the fuel feedstock [92]. Thus, steam in an amount greater than required for stoichiometric reaction (3.34) is supplied.

#### 4. Discussion and potential impact of integrated BG-SOFC process

Biomass gasification is a potential technology for producing low-medium calorific gas from biomass. As shown in Table 4, gasification of biomass produces a gas consisting mainly of  $H_2$ , CO,  $CO_2$ ,  $CH_4$ ,  $N_2$  and light hydrocarbons. The composition of the product gas varies depending on the biomass used, the gasification technology (fluidized bed, fixed Bed) and the medium used during gasification (air, steam, oxygen). Gasification processes using air as the gasification medium produces a fuel gas, with  $N_2$  content up to 50 vol%. Steam gasification produces a gas richer in  $H_2$  (35–45 vol%) and CO (20–30 vol%) and with a low  $N_2$  content (3–4 vol.%). Steam gasification of biomass is therefore suitable for an integrated system with SOFC.

SOFCs have the potential to become a major technology for power generation in the coming decades, due to high efficiencies (45–60% of the fuel's LHV compared to 30–40% of conventional systems) and extremely low  $NO_x$  and  $C_xH_y$  emissions (1/300 compared to coal-based plants). Conversion efficiencies are expected up to 45% (BG-SOFC) based on modeling analyses. The accurate prediction of SOFC operating conditions is important for attaining high efficiencies and successfully integrating both systems (BG-SOFC). The spectrum of possible operating conditions can be determined based on the performance characteristics of the fuel cell. These characteristics will allow us to determine a set of operating conditions (temperature, pressure, inlet compositions) for optimal performance.

The high operating temperature (600–1000 °C) allows SOFCs to operate on a range of fuels (pipeline natural gas, gasified biomass or coal, anaerobic biogas, reformed hydrocarbons etc.), a flexibility which promotes their commercialization chances, since pure  $H_2$  is not readily available. Furthermore, it renders them as ideal candidates for high-quality heat cogeneration, which can be used for heating purposes or in bottoming thermal engines for additional electric power generation (overall efficiencies, of SOFC-gas turbine combined cycles, exceed 70%). Power density and fuel utilization determine the overall efficiency of the cell, while these parameters are readily affected by the operational cell voltage. In the case of the wide range of biogas compositions, the dilution of  $H_2/CO/C_xH_y$  combustible agent, results in a decrease of the voltage and of the cells power density. SOFCs can tolerate a wide variety of  $H_2/CO/C_xH_y$  compositions, but the performance optimization may require significant operating condition and/or system design changes.

The combination of biomass with fuel cells emerged only recently, as a beneficiary candidate for decentralized and renewable heat and power cogeneration. In the frame of a

project carried out in our laboratory, concerning sustainable development and sustainable water management of non-European Mediterranean countries, it has been shown that modular biomass gasification/SOFC systems could provide renewable energy for desalination systems.

As it is known, in non-European Mediterranean countries, agriculture provides the living basis for most of the rural population (over 10% of the regional workforce) and consumes over 80% of the scarce water resources. Sustainable water management in rural areas is inevitable to pass through the exploitation of the large marginal water sources of the region, located at the subsoil of semi-arid areas, which surrounds fertile planes and are usually subjected to cereal-weed/fodder fallow rotation. Marginal water pumping and purification/desalination requires an adequate energy supply, while biomass is widely recognized as the most suitable basis to provide this energy.

Sufficient amounts of cereal, cotton, corn, olive, coffee or palm tree residues are available in these areas, while the climatic conditions are favorable for energy crops cultivations, which can be irrigated with brackish water or even harvested on local rain-fed conditions.

In this context, fuel cells, due to their high efficiency (over 70% in combined cycles compared to almost 35% of conventional thermal engines), offer the perspective of the highly efficient utilization of the largely unexploited biogas issued from biomass gasification potential. Among various types of fuel cells, SOFCs exhibit advanced fuel flexibility, compared to low-temperature ones, primarily because CO poisons low-temperature electrocatalysts, whereas it acts as a fuel in SOFCs.

Our on-going project aiming to examine the effectiveness of incorporating an SOFC in conventional gasification–turbine process has justified that the SOFC can substantially upgrade the efficiency of the biomass-to-energy conversion and has resulted (from the theoretical analyses concerning an ideal case of thermodynamic efficiencies under no thermal losses operation) in that SOFC contribution to the overall power generation usually exceeds 60%. Furthermore, the overall electrical efficiency of the integrated process can, ideally, overcome 60% of the heating value of the biomass feed, whereas conventional technologies, like turbines, can only randomly reach 40% of the heat supplied to their inlet.

## **5. Conclusions**

Biomass gasification is a potential technology for producing low-medium calorific gas from biomass.

High gasification temperature contributes to more hydrogen production, but decreases also the gas-heating value.

Compared to biomass air gasification, the introduction of steam improved gas quality. However, excessive steam would lower gasification temperature and so degrade fuel gas quality.

The conjunction of biomass gasification with SOFCs seemed to be a promising and forthcoming possibility for electricity and heat cogeneration along with profound environmental and socioeconomic benefits. Steam gasification exhibits enhanced conversions to hydrogen, and it is considered to be superior to the conventional one since it evolves steam's hydrogen in the integrated.



The conjunction of SOFCs with steam gasifiers can contribute significantly to overcome the endothermicity of the latest and bypass the capital costs of the intermediate biogas-reforming stage. The inherent ability of SOFCs system to keep the anode and cathode exhaust gases separate allows the exploitation of SOFC over-fueling (low utilization) and adding downstream operations for the anode exhaust gases, such as a gas turbine.

The drive for using biofuels in SOFCs, in remote rural areas, is regarded to be both environmental and financial, since connection to the grid can be expensive in such areas where biogas can be produced on site with no significant extra costs. Bio-energy-based water-treatment plants, which are suitable and cost effective for decentralized applications, coincide interesting conditions in these emerging water-supply markets.

Despite the benefits of fuel cells, their potential to become a viable option depends foremost on the capital cost of the system. Fuel cell need to be cost-competitive compared to conventional power-generation systems.

## Acknowledgments

The authors acknowledge the General Secretariat for Research and Development (GSRT) of Greece and EC for the financial support under the PYTHAGORAS II program.

## References

- [1] EG-G Services. Fuel cell handbook, 6th ed. Parsons Inc., Science Applications International Corporation, 2002.
- [2] Larminie J, Dicks A. Fuel cell systems explained. New York: Wiley; 2002.
- [3] Lymperopoulos N. Fuel cell and their application in bio-energy. Project technical assistant framework contract (EESD Contract No.: NNE5-PTA-2003-003/1), 2002.
- [4] Dayton DC, Ratcliff M, Bain R. Fuel cell integration—a study of the impacts of gas quality and impurities. NREL Technical Report NREL/MP-510-30298, June 2001.
- [5] Yi Y, Rao AD, Brouwer J, Samuelsen GS. Fuel flexibility study of an integrated 25 kW SOFC reformer system. *J Power Sources* 2005;144:67–76.
- [6] Marsano F, Magistri L, Bozzolo M, Tarnowski O. Influence of fuel composition on solid oxide fuel cell hybrid system layout and performance. Vienna, Austria: ASME Turbo Expo GT2004-53853.
- [7] Eguchi K, Kojo H, Takeguchi T, Kikuchi R, Sasaki K. Fuel flexibility in power generation by solid oxide fuel cells. *Solid State Ionics* 2002;152–153:411–6.
- [8] Coutelieris FA, Douvartzides S, Tsiakaras P. The importance of the fuel choice on the efficiency of a solid oxide fuel cell system. *J Power Sources* 2003;123(2):200–5.
- [9] Douvartzides SL, Coutelieris FA, Demin AK, Tsiakaras PE. Fuel options for solid oxide fuel cells: a thermodynamic analysis. *AIChE J* 2003;49(1):248–57.
- [10] Singhal SC. Advances in solid oxide fuel cell technology. *Solid State Ionics* 2000;135:305–13.
- [11] Alderucci V, Antonucci PL, Maggio G, Giordano N, Antonucci V. Thermodynamic analysis of SOFC fuelled by biomass derived gas. *Int J Hydrogen Energy* 1993;19(4):369–76.
- [12] Staniforth J, Kendall K. Biogas powering a small tubular SOFC. *J Power Sources* 1998;71:275.
- [13] van Herle J, Membrez Y, Bucheli O. Biogas as a fuel source for SOFC cogeneratos. *J Power Sources* 2004;127:300.
- [14] Zhu B, Bai X, Chen G, Yi W, Burcell M. Fundamental study on biomass fuelled ceramic fuel cells. *Int J Energy Resour* 2002;26:57.
- [15] Omosun, Bauen A, Brandon N, Adjiman C, Hart D. Modelling system and costs of two biomass fuelled SOFC systems. *J Power Sources* 2004;131:96.
- [16] Van herle J, Marechal F, Leuenderger S, Favrat D. Energy balance model of a SOFC cogenerator operated with biogas. *J Power Sources* 2005;118:375.

- [17] Van herle J, Marechal F, Leuenderger S, Membrez Y, Bucheli O, Favrat D. Process flow model of SOFC system supplied with sewage biogas. *J Power Sources* 2004;131:127.
- [18] Sammes N, Bove Y. Design and fabrication of a 100 kW anode supported micro-tubular SOFC stack. *J Power Sources* 2005;145:428.
- [19] Brown NM, Primdahl S, Moggensen M. *J Electrochem Soc* 2000;147:475.
- [20] Singh D, Pacheco EH, Hutton PN, Patel N, Mann MD. Carbon deposition in an SOFC fueled by tar-laden biomass gas: a thermodynamic analysis. *J Power Sources* 2005;142:194–9.
- [21] Aguiar P, Chadwick D, Kershenbaum L. Modelling of an indirect internal reforming solid oxide fuel cell. *Chem Eng Sci* 2002;57:1665–77.
- [22] Van Swaaij WPM, van den Aarsen FG, Bridgewater AV, Heesink ABM. A review of biomass gasification'. Report to the Commission of the European Communities, DG XII, 1994.
- [23] Lindman N. Proceedings of conference on energy from biomass and wastes V, Lake Buena Vista. Amsterdam: Elsevier; 1981. p. 89 (INCO Specific Measures Guide for Proposers for STREP Call FP6-2004-INCO-DEV-3, FP6-2004-INCO-MPC-3, Publication date: 17/12/2004 62).
- [24] Sutton D, Kelleher B, Ross JRH. Review of literature on catalysts for biomass gasification. *Fuel Process Technol* 2001;73:155–73.
- [25] McKendry P. Energy production from biomass (part1): Overview of biomass. *Bioresour Technol* 2002;83:37–46.
- [26] Encinar JM, Gonzalez JF, Gonzalez J. Steam gasification of cynara cardunulus L: influence of variables. *Fuel Process Technol* 2002;75:27–43.
- [27] Mansaray KG. Gasification of rice husk in fluidized bed reactor. PhD thesis, Dalhousie University, Nova Scotia, Canada, 1998.
- [28] Ioannidou O, Zabaniotou A. Agricultural residues as precursors for activated carbon production—a review. *Renew Sustain Energy Rev*, in press, Corrected proof, doi:10.1016/j.rser.2006.03.013.
- [29] Skoulou V, Zabaniotou A. Investigation of agricultural and animal wastes in Greece and their allocation to potential application for energy production. *Renew Sustain Energy Rev*, in press, Corrected proof, doi:10.1016/j.rser.2005.12.011.
- [30] Maniatis K. Progress in biomass gasification: an overview. Directorate General for Energy and Transport.
- [31] Bridgewater AV. Renewable fuels and chemicals by thermal processing of biomass. *Chem Eng J* 2003; 91:87–102.
- [32] McKendry P. Energy production from biomass (part 2): conversion technologies. *Bioresour Technol* 2002;83:47–54.
- [33] McKendry P. Energy production from biomass (part 3): gasification technologies. *Bioresour Technol* 2002; 83:55–63.
- [34] Hofbauer H, Rauch R, Bosch K, Koch R, Aichernig C. Biomass CHP plant Güssing—a success story. In: Bridgewater AV, editor. *Pyrolysis and gasification of biomass and waste*. Newbury, UK: CPL Press; 2003.
- [35] Knoef HAM. Inventory of biomass gasifier manufacturers and installations. Final report to European Commission, Contract DIS/1734/98-NL, Biomass Technology Group B.V., University of Twente, Enschede, 2000 (see <http://btgs1.ct.utwente.nl/>).
- [36] van Paasen SVB, Kiel JHA. Tar formation in a fluidized bed gasifier. Report ECN-C-04-013, ECN, March 2004.
- [37] Delgado J, Aznar MP. Biomass gasification with steam in fluidized bed: effectiveness of CaO, MgO, and CaO–MgO for hot raw gas cleaning. *Ind Eng Chem Res* 1997;36:1535–43.
- [38] Delgado J, Aznar MP, Corella J. Calcined dolomite, magnesite and calcite for cleaning hot gas from a fluidized bed biomass gasifier with steam: life and usefulness. *Ind Eng Chem Res* 1996;35:3637–43.
- [39] Aznar MP, Caballero MA, Gil J, Martin JA, Corella J. Commercial steam reforming catalysts to improve biomass gasification with steam–oxygen mixtures. 2. Catalytic tar removal. *Ind Eng Chem Res* 1998; 37:2668–80.
- [40] Gil J, Corella J, Aznar MP, Caballero MA. Biomass gasification in atmospheric and bubbling fluidized bed: effect of the type of gasifying agent on the product distribution. *Biomass Bioenergy* 1999;17:389–403.
- [41] Rapagna S, Jand N, Kiennemann A, Foscolo PU. Steam gasification of biomass in a fluidized-bed of olivine particles. *Biomass Bioenergy* 2000;19:187–97.
- [42] Spliethoff H. Status of biomass gasification for power production, IFRF Combustion Journal, Article No 200109, November 2001.
- [43] Sadaka SS, Ghaly AE, Sabbah MA. Two phase biomass air-steam gasification model for fluidized bed reactors. Part I: model development. *Biomass Bioenergy* 2002;22:439–62.

- [44] Sadaka SS, Ghaly AE, Sabbah MA. Two phase biomass air–steam gasification model for fluidized bed reactors. Part II: model sensitivity. *Biomass Bioenergy* 2002;22:463–77.
- [45] Sadaka SS, Ghaly AE, Sabbah MA. Two phase biomass air–steam gasification model for fluidized bed reactors. Part III: model validation. *Biomass Bioenergy* 2002;22:479–87.
- [46] Lv PM, Xiong ZH, Chang J, Wu CZ, Chen Y, Zhu JX. An experimental study on biomass air–steam gasification in a fluidized bed. *Bioresour Technol* 2004;95:95–101.
- [47] Franco C, Pinto F, Gulyurtlu I, Cabrita I. The study of reactions influencing the biomass steam gasification process. *Fuel* 2003;82:835–42.
- [48] Walawender WP, Hoveland DA, Fan LT. *Ind Eng Chem Process Des Dev* 1985;24:897.
- [49] Corella J, Aznar M, Delagdo J, Aldea E. *Ind Eng Chem Res* 1991;30:2252–62.
- [50] Wang Y, Knoshita CM. *Solar Energy* 1992;49:153–8.
- [51] Chan SH, Ho HK, Tian Y. Modelling of simple hybrid SOFC and gas turbine power plant. *J Power Sources* 2002;109:111–20.
- [52] Chan SH, Ho HK, Tian Y. Modelling for part-load operation of SOFC-gas turbine hybrid power plant. *J Power Sources* 2003;114:213–27.
- [53] Chan SH, Ho HK, Tian Y. Multi-level modelling of SOFC-gas turbine hybrid system. *Int J Hydrogen Energy* 2003;28:889–900.
- [54] Costamagna P, Selimovic A, Del Borghi M, Agnew G. Electrochemical model of the integrated planar solid oxide fuel cell (IP-SOFC). *Chem Eng J* 2004;102:61–9.
- [55] Stiller C, Thorud B, Seljebo S, Mathisen O, Karoliusen H, Bolland O. Finite volume modelling and hybrid-cycle performance of planar and tubular solid oxide fuel cells. *J Power Sources* 2005;141:227–40.
- [56] Palsson J, Selimovic A, Sjunnesson L. Combined solid oxide fuel cell and gas turbine systems for efficient power and heat generation. *J Power Sources* 2000;86:442–8.
- [57] Pacheco EH, Mann MD, Hutton PN, Singh D, Martin KE. A cell-level model for a solid oxide fuel cell operated with syngas from a gasification process. *Int J Hydrogen Energy* 2005;30:1221–33.
- [58] Vasileiadis S, Ziaka-Vasileiadou Z. Biomass reforming process of an integrated solid oxide-fuel cell power generation. *Chem Eng Sci* 2004;59(22–23):4853–9.
- [59] Ghosh S, De S. Energy analysis of a cogeneration plant using coal gasification and solid oxide fuel cell. *Energy* 2006;31:345–63.
- [60] Aravind PV, Ouweltjes JP, de Heer E, Woudstra N, Rietveld G. Impact of biosyngas and its properties on SOFC anodes, ECN-RX-05-117, 2005.
- [61] Panopoulos KD, Fryda LE, Karl J, Poulou S, Kakaras E. High temperature solid oxide fuel cell integrated with novel allothermal biomass gasification Part I: Modelling and feasibility study. *J Power Sources* 2006;159:570–5.
- [62] Panopoulos KD, Fryda LE, Karl J, Poulou S, Kakaras E. High temperature solid oxide fuel cell integrated with novel allothermal biomass gasification Part II: exergy analysis. *J Power Sources* 2006;159:586–94.
- [63] Baron S, Brandon N, Atkinson A, Steele B, Rudkin R. The impact of wood derived gasification gases on Ni-CGO anodes in intermediate temperature solid oxide fuel cells. *J Power Sources* 2004;126:58–66.
- [64] Chen F, Zha A, Dong J, Liu M. Pre-reforming of propane for low temperature SOFCs. *Solid State Ionics* 2004;166:269–73.
- [65] Achenbach E, Riensche E. Methane/steam reforming kinetics for solid oxide fuel cells. *J Power Sources* 1994;52:228–83.
- [66] Matsuzaki NY, Yasuda I. *J Electrochem Soc* 2000;147:1630.
- [67] Jiang Y, Virkar A. *J Electrochem Soc* 2003;150:A942.
- [68] Costa-Nunes O, Gorte R, Vohs J. Comparison of the performance of Cu–CeO<sub>2</sub>–YSZ and Ni-YSZ composite SOFC anodes with H<sub>2</sub>, CO and syngas. *J Power Sources* 2005;141:241.
- [69] Vielstich W, Lamm A, Gasteiger H. *Handbook of fuel cells, fundamentals technology and applications*, vol. II. New York: Wiley; 2003.
- [70] Collins J, Stimming U. In: Wieckowski A, Savinova E, Vayenas C, editors. *Catalysis and electrocatalysis in nanoparticles*. New York: Marcel Decker Inc.; 2003. p. 531.
- [71] Kim H, Vohs J, Gorte R. *J Chem Soc Chem Commun* 2001:2334.
- [72] Lee S-I, Vohs J, Gorte R. *J Electrochem Soc* 2004;151:A1319.
- [73] Barbucci A, Carpanese P, Cerisola G, Viviani M. Electrochemical investigation of mixed ionoc/electronic cathodes for SOFCs. *Solid State Ionics* 2005;176:1753.
- [74] Wang W, Mogensen M. High-performance lanthanum-ferrite-based cathode for SOFC. *Solid State Ionics* 2005;176:457.

- [75] Costamagna P, Costa P, Antonucci V. Micro-modelling of solid oxide fuel cell electrodes. *Electrochem Acta* 1998;43(3–4):375–94.
- [76] Chan SH, Xia ZT. Anode micro model of solid oxide fuel cell. *J Electrochem Soc* 2001;148(4):A388–94.
- [77] Divisek J, Jung R, Vinke IC. Structure investigations of SOFC anode cermets. Part II: electrochemical and mass transport properties. *J Appl Electrochem* 1999;29:165–70.
- [78] Kim JW, Virkar AV, Fung KZ, Mehta K, Singhal SC. Polarization effects in intermediate temperature, anode-supported solid oxide fuel cells. *J Electrochem Soc* 1999;146(1):69–78.
- [79] Sunde S. Simulations of composites electrodes in fuel cells. *J Electroceramics* 2000;5(2):153–82.
- [80] Chan SH, Khor KA, Xia ZT. A complete polarization model of a solid oxide fuel cell and its sensitivity to the change of cell component thickness. *J Power Sources* 2001;93:130–40.
- [81] Zhu H, Kee RJ. A general mathematical model for analyzing the performance of fuel-cell membrane-electrode assemblies. *J Power Sources* 2003;117:61–74.
- [82] Yakabe H, Hishinuma M, Uratani M, Matsuzaki Y, Yasuda I. Evaluation and modelling of performance of anode-supported solid oxide fuel cell. *J Power Sources* 2000;86:423–31.
- [83] Lehnert W, Meusinger J, Thom F. Modelling of gas transport phenomena in SOFC anodes. *J Power Sources* 2000;87:57–63.
- [84] Achenbach E. Three-dimensional and time-dependent simulation of a planar solid oxide fuel cell stack. *J Power Sources* 1994;49:333–48.
- [85] Yakabe H, Ogiwara T, Hishinuma M, Yasuda I. 3-D model calculation for planar SOFC. *J Power Sources* 2001;102:144–54.
- [86] Iwata M, Hikosaka T, Morita M, Iwanari T, Ito K, Onda K, et al. Performance analysis of planar-type unit SOFC considering current and temperature distributions. *Solid State Ionics* 2000;132:297–308.
- [87] Chan SH, Xia ZT. Polarization effects in electrolyte/electrode-supported solid oxide fuel cells. *J Appl Electrochem* 2002;32:339–47.
- [88] Athanasiou C, Coutelieres F, Vakouftsi E, Skoulou V, Antonakou E, Marnellos G, Zabaniotou A. From biomass to electricity through integrated gasification/SOFC system optimization and energy balance. *Int J Hydrogen Energy* 2007;32(3):337–42.
- [89] Aravind PV, Woudstra N, Ouweltjes JP, Andries J, de Jong W, Rietveld G, Spliethoff H. Integration of solid oxide fuel cells with biomass gasifiers, ECN-RX-05-086, 2005.
- [90] Chan SH, Low CF, Ding OL. Energy and exergy analysis of simple solid oxide fuel cell power systems. *J Power Sources* 2002;103:188–200.
- [91] Song C. Fuel processing for low-temperature and high-temperature fuel cells. Challenges, and opportunities for sustainable development in the 21st century. *Catal Today* 2002;77:17–49.
- [92] Rostrup-Nielsen JR. In: Anderson JR, Boudart M, editors. Catalytic steam reforming, Catalysis science and technology, vol. 5. New York: Springer Verlag; 1984.